

Devil's lenses

Juan A. Monsoriu^{1*}, Walter D. Furlan², Genaro Saavedra², and Fernando Giménez³

¹Departamento de Física Aplicada, Universidad Politécnica de Valencia, E-46022 Valencia, Spain

²Departamento de Óptica, Universitat de València, E-46100 Burjassot, Spain

³Departamento de Matemática Aplicada, Universidad Politécnica de Valencia, E-46022 Valencia, Spain

*Corresponding author: jmonsori@fis.upv.es

Abstract: In this paper we present a new kind of kinoform lenses in which the phase distribution is characterized by the “devil’s staircase” function. The focusing properties of these fractal DOEs coined *devil’s lenses* (DLs) are analytically studied and compared with conventional Fresnel kinoform lenses. It is shown that under monochromatic illumination a DL give rise a single fractal focus that axially replicates the self-similarity of the lens. Under broadband illumination the superposition of the different monochromatic foci produces an increase in the depth of focus and also a strong reduction in the chromaticity variation along the optical axis.

©2007 Optical Society of America

OCIS codes: (050.1940) diffraction; (050.1970) diffractive optics;

References and Links

1. J. Courtial and M. J. Padgett, “Monitor-outside-a-monitor effect and self-similar fractal structure in the eigenmodes of unstable optical resonators,” *Phys. Rev. Lett.* **85**, 5320-5323 (2000).
2. O. Trabocchi, S. Granieri, and W. D. Furlan, “Optical propagation of fractal fields. Experimental analysis in a single display,” *J. Mod. Opt.* **48**, 1247-1253 (2001).
3. M. Lehman, “Fractal diffraction gratings built through rectangular domains,” *Opt. Commun.* **195**, 11-26 (2001).
4. J. G. Huang, J. M. Christian, and G. S. McDonald “Fresnel diffraction and fractal patterns from polygonal apertures,” *J. Opt. Soc. Am. A* **23**, 2768-2774 (2006).
5. G. Saavedra, W. D. Furlan, and J. A. Monsoriu, “Fractal zone plates,” *Opt. Lett.* **28**, 971-973 (2003).
6. J.A. Monsoriu, G. Saavedra, and W.D. Furlan, “Fractal zone plates with variable lacunarity,” *Opt. Express* **12**, 4227-4234 (2004). <http://www.opticsinfobase.org/abstract.cfm?URI=oe-12-18-4227>
7. J. A. Davis, L. Ramirez, J. A. Rodrigo Martín-Romo, T. Alieva, and M. L. Calvo, “Focusing properties of fractal zone plates: experimental implementation with a liquid-crystal display,” *Opt. Lett.* **29**, 1321-1323 (2004).
8. H.-T. Dai, X. Wang, K.-S. Xu, “Focusing properties of fractal zone plates with variable lacunarity: experimental studies based on liquid crystal on silicon,” *Chin. Phys. Lett.* **22**, 2851-2854 (2005).
9. S. H. Tao, X.-C. Yuan, J. Lin, and R. Burge, “Sequence of focused optical vortices generated by a spiral fractal zone plates,” *Appl. Phys. Lett.* **89**, 031105 (2006).
10. C. Martelli and J. Canning, “Fresnel Fibres with Omnidirectional Zone Cross-sections,” *Opt. Express* **15**, 4281-4286 (2007).
11. F. Giménez, J. A. Monsoriu, W. D. Furlan, and A. Pons, “Fractal Photon Sieves,” *Opt. Express* **14**, 11958-11963 (2006). <http://www.opticsinfobase.org/abstract.cfm?URI=oe-14-25-11958>
12. J. A. Jordan, P. M. Hirsch, L. B. Lesem, and D. L. Van Rooy, “Kinoform lenses,” *Appl. Opt.* **9**, 1883-1887 (1970)
13. D. R. Chalice, “A characterization of the Cantor function,” *Amer. Math. Monthly* **98**, 255-258 (1991).
14. F. Doveil, A. Macor, and Y. Elskens, “Direct observation of a devil’s staircase in wave-particle interaction,” *Chaos* **16**, 033130 (2006).
15. M. Hupalo, J. Schamalian, and M. C. Tringides, “Devil’s staircase in Pb/Si(111) ordered phases,” *Phys. Rev. Lett.* **90**, 216106 (2003).
16. Y. F. Chen, T. H. Lu, K. W. Su, and K. F. Huang, “Devil’s staircase in three-dimensional coherent waves localized on Lissajous parametric surfaces,” *Phys. Rev. Lett.* **96**, 213902 (2006).
17. Y. Han, L. N. Hazra, and C. A. Delisle, “Exact surface-relief profile of a kinoform lens from its phase function,” *J. Opt. Soc. Am. A* **12**, 524-529 (1995).
18. M. J. Yzuel and J. Santamaria, “Polychromatic Optical Image.Diffraction Limited System and Influence of the Longitudinal Chromatic Aberration,” *Opt. Acta* **22**, 673-690 (1975).

1. Introduction

Fractal optics is nowadays a well established branch of optics that covers several research topics including the analysis of the properties of laser beams having fractal spatial and temporal structure [1]; the study of the properties of fractal optical fields [2-4], and the theory and applications of fractal diffractive lenses. In this context, we have proposed fractal zone plates (FraZPs) which are binary amplitude zone plates with fractal profile along the square of the radial coordinate [5,6]. FraZP have deserved the attention of several experimental research groups working in diffractive optics [7,8] and inspired the invention of other photonic structures such as spiral fractal zone plates [9], optical fibers with fractal cross section [10] and fractal photon sieves [11].

Since the diffraction efficiency of the diffractive optical elements (DOEs) is crucial for certain practical applications, in this work we introduce the concept of fractal kinoform lenses, i.e. blazed zone plates [12] with fractal structure. The surface relief of this new kind of DOEs is obtained using the *devil's staircase* function [13]. Because of the form of its generating function we called these new kind of DOEs "Devil's Lenses" (DLs). The devil's staircase function, that is related to the standard Cantor set, also appears in several areas of physics, as for instance, in wave-particle interactions [14], in crystal growth [15], and in the mode locking of the 3D coherent states in high-Q laser cavities [16].

DLs design is formally presented in this paper and an analytical expression for the phase profile is derived. As blazed DOEs, DLs drives most of the incoming light into one single main fractal focus, improving in this way the efficiency of FraZPs. The focusing properties of DLs are studied by computing the intensity distribution along the optical axis and the evolution of the diffraction patterns transversal to the propagation direction. Moreover, since most of applications of diffractive lenses are related with broadband illumination sources, the intensity distributions near the focus is evaluated by means of polychromatic merit functions. In order to assess our proposal all the results are compared with those obtained with conventional Fresnel kinoform lenses.

2. Devil's lenses design

We will call DL to any rotationally symmetric diffractive lens whose phase profile is designed from a devil's staircase function. A standard example of a devil's staircase is the Cantor function, which can be generated from any given Cantor set (CS). The first step in the CS construction procedure, consists in defining a straight-line segment of unit length called *initiator* (stage $S=0$). Next, at stage $S=1$, the *generator* of the set is constructed by dividing the segment into m equal parts of length $1/m$ and removing some of them. Then, this procedure is continued at the subsequent stages, $S=2, 3, \dots$. Without loss of generality, let us consider the triadic CS shown in the upper part of Fig. 1(a). In this case $m=3$ and it is easy to see that, at stage S there are 2^S segments of length 3^{-S} with 2^S-1 disjoint gaps intervals $[p_{S,l}, q_{S,l}]$, with $l=1, \dots, 2^S-1$. Based on this fractal structure, in this case the devil's staircase Cantor function [13], can be defined in the interval $[0,1]$ as

$$F_S(x) = \begin{cases} \frac{l}{2^S} & \text{if } p_{S,l} \leq x \leq q_{S,l} \\ \frac{1}{2^S} \frac{x - q_{S,l}}{p_{S,l+1} - q_{S,l}} + \frac{l}{2^S} & \text{if } q_{S,l} \leq x \leq p_{S,l+1} \end{cases}, \quad (1)$$

being $F_S(0)=0$ and $F_S(1)=1$. For example, for $S=3$ [see Fig. 1(a)], the triadic Cantor set presents seven gaps limited by the following positions inside the unit length: $[1/27, 2/27]$, $[3/27, 6/27]$, $[7/27, 8/27]$, $[9/27, 18/27]$, $[19/27, 20/27]$, $[21/27, 24/27]$, and $[25/27, 26/27]$. The steps of the devil's staircase, $F_S(x)$, take in the above intervals the constant values $l/2^3$ with $l=1, \dots, 7$. In between these intervals the continuous function is linear.

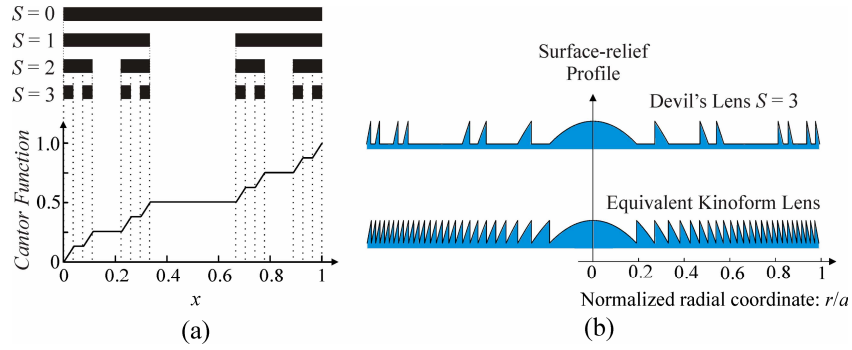


Fig. 1. (a) Triadic Cantor set for $S=1$, $S=2$, and $S=3$. The structure for $S=0$ is the initiator and the one corresponding to $S=1$ is the generator. The Cantor function or Devil's staircase, $F_S(x)$, is shown under the corresponding Cantor set for $S=3$. (b) Convergent DL at stage of growth $S=3$ and the equivalent kinoform Fresnel lens.

From $F_S(x)$ we define the corresponding DL as a circularly symmetric DOE with a phase profile which follows the Cantor function at a given stage, S . At the gap regions defined by the Cantor set the phase shift is $-l2\pi$, with $l=1, \dots, 2^S-1$. Thus, the convergent DL transmittance is defined by

$$q(\zeta) = q_{DL}(\zeta, S) = \exp[-i 2^{S+1} \pi F_S(\zeta)], \quad (2)$$

where

$$\zeta = (r/a)^2 \quad (3)$$

is the normalized quadratic radial variable and a is the lens radius. Thus, the phase variation is quadratic in each zone of the lens. The surface-relief profile, $h(r)$, of the DL corresponding to the above phase function can be obtained from the relation [17]

$$h_{DL}(r) = \text{mod}_{2\pi} \left\{ -2^{S+1} \pi F_S \left(\frac{r^2}{a^2} \right) \right\} \frac{\lambda}{2\pi(n-1)}, \quad (4)$$

where $\text{mod}_{2\pi}[\phi(r)]$ is the phase function $\phi(r)$ modulo 2π , n is the refractive index of the optical material used for constructing the lens, and λ is the wavelength of the light.

The upper part of Fig. 1(b) shows the profile of a convergent DL generated using Eq. (4). For comparison we have depicted at the lower part of the same figure the profile corresponding to a conventional Fresnel kinoform lens of the same focal length. It is instructive to note that the DL can be understood as a conventional kinoform lens but with some missing phase zones.

3. Focusing properties of a DL

Since we will consider DOEs whose minimum feature size is much greater than the wavelength of incident light we will use the scalar diffraction to evaluate their performance. In fact, we will show that even for the lower values of S the distinctive features of DLs are evident. Then, within that approximation, the irradiance at a given point in the diffraction pattern produced by a general rotationally invariant pupil with a transmittance $p(r_o)$ is given by

$$I(z, r) = \left(\frac{2\pi}{\lambda z} \right)^2 \left| \int_0^a p(r_o) \exp\left(-i \frac{\pi}{\lambda z} r_o^2\right) J_0\left(\frac{2\pi r_o r}{\lambda z}\right) r_o \, dr_o \right|^2; \quad (5)$$

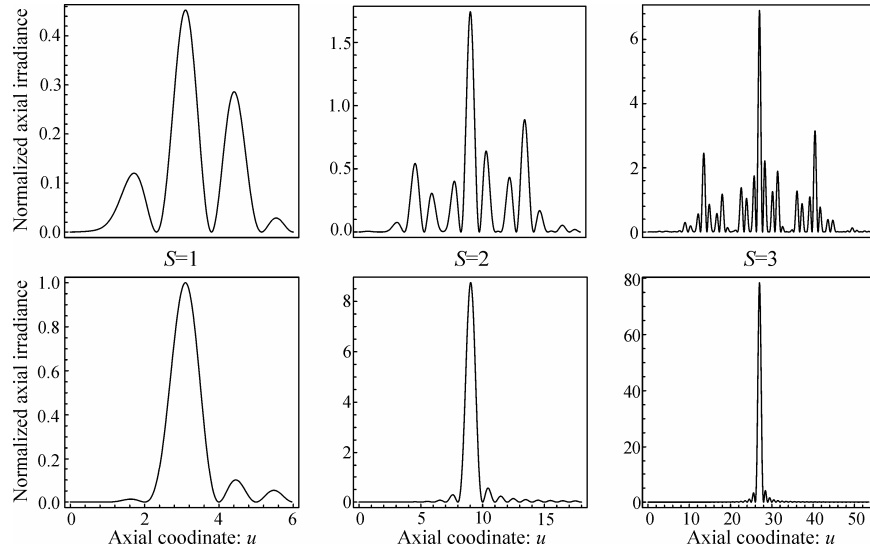


Fig. 2. Normalized irradiance vs. the axial coordinate u obtained for aDL at three stages of growth (upper part) and for its associated Fresnel kinoform lens (lower part).

where z is the axial distance from the pupil plane, r has its origin at the optical axis, and λ is the wavelength of the incident monochromatic plane wave. If the pupil transmittance is defined in terms of the normalized variable in Eq. (3), the irradiance can be expressed as the Hankel transform of the pupil function,

$$I(u, v) = 4\pi^2 u^2 \left| \int_0^1 q(\zeta) \exp(-i2\pi u\zeta) J_0(4\pi\sqrt{\zeta}uv) d\zeta \right|^2, \quad (6)$$

where $q(\zeta)=p(r_o)$. In Eq. (6), $u=a^2/2\lambda z$ and $v=r/a$ are the reduced axial and transverse coordinates, respectively. If we focus our attention to the values the irradiance takes along the optical axis, then $v=0$, and Eq. (6) reads

$$I_0(u) = 4\pi^2 u^2 \left| \int_0^1 q(\zeta) \exp(-i2\pi u\zeta) d\zeta \right|^2. \quad (7)$$

Thus, the axial irradiance can be expressed in terms of the Fourier transform of the mapped pupil function $q(\zeta)$. Using Eq. (2) for the transmittance corresponding to a DL and taking into account that one of the features of self-similar structures is that the dimensionality of the structure appears in its power spectrum [5], then Eq. (7) predicts that a DL will produce an irradiance along the optical axis with a fractal profile that resembles the structure of the DL itself. To show this fact explicitly, the axial irradiance of the DL computed for different stages of growth S is shown in Fig. 2. The irradiance of the associated kinoform Fresnel lens is shown in the same figure for comparison. Note that the scale in the axial coordinate for each value of S is different. It can be seen that the axial position of the focus of the Fresnel kinoform lens and the central lobe of the DL focus both coincide at the normalized distance $u=3^S$. Thus, from the change of variables adopted in Eq.(6) the focal length of the DL can be expressed as

$$f_s = \frac{a^2}{2\lambda 3^s}. \quad (8)$$

As expected, the axial response for the DL exhibits a single major focus and a number of subsidiary focal points surrounding it, producing a the focus region with a characteristic

fractal profile. In fact, the three patterns in the upper part of Fig. 2 are self-similar, i.e., as S becomes larger an increasing number of zeros and maxima are encountered, which are scale invariant over dilations of factor $\gamma=3$. The axial intensity distributions corresponding to the ZPs of low level involve the curves of the upper ones. This focalization behavior, which is here demonstrated that DLs satisfy, is, in fact, an exclusive feature of FraZPs and it was called *the axial scale property* [5]. Interestingly the main focus of the DLs presents a certain degree of axial superresolution. This effect is particularly evident from the comparison of the upper and lower parts in Fig.2 for the irradiances corresponding to $S=2$ and $S=3$.

4. Evolution of the diffraction patterns produced by a DL

The distribution of the diffracted energy, not only in the axial direction but over the whole transverse plane is of interest for the prediction of the imaging capabilities of the DLs. Thus, a two-dimensional analysis of the diffracted intensities is required. Equation (6) has been used to calculate the evolution of the diffraction patterns for a DL from near to far field. The result obtained for $S=2$ is shown in the animated Fig. 3 (left). For comparison, the right half of this figure shows the transverse patterns produced by a Fresnel kinoform lens of the same focal length. The counter in this figure shows the value of the normalized distance (z/f) from the lens that corresponds to each transversal pattern. In each frame the diffraction pattern is represented within the range $|x/a|<0.5$, $|y/a|<0.5$ of the transverse coordinates and the intensities are normalized to the maximum value at each transverse plane. In this way, the relative intensity at the main focus of both lenses ($z/f=1$) can be directly compared. From this figure it can be noted that the axial secondary maxima provided by the DL results in an effective increase of the depth of focus. The intensity given by the kinoform Fresnel lens at those far planes is almost zero.

Of particular interest are the intensities at transverse planes corresponding to the different maxima and minima of the axial irradiance. These are depicted in Fig. 4 together with their relative intensities. Note that the predicted minima are characterized by a concentric doughnut form.

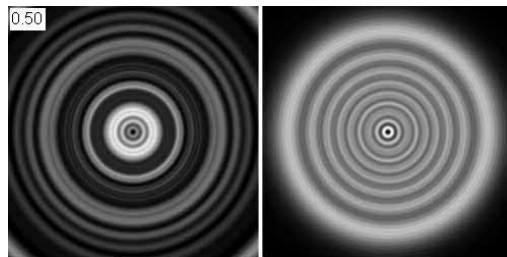


Fig. 3. (387 kB) Evolution of the transverse diffraction patterns generated by a $S=2$ DL, (left), and a Fresnel kinoform lens of the same focal length.

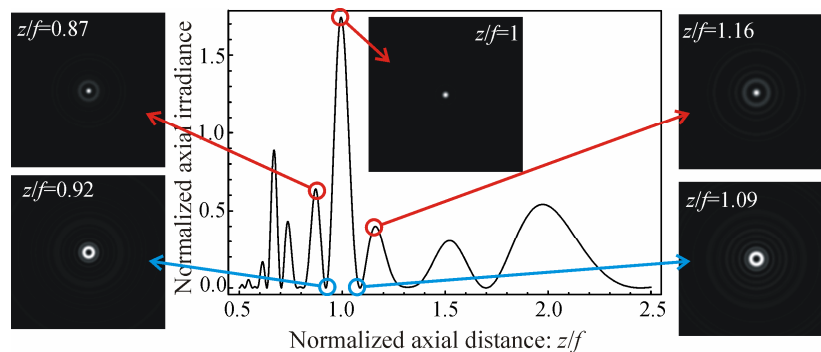


Fig. 4. Transverse diffraction patterns around the principal focus of a DL with $S=2$. The normalized axial distance is given by $z/f_2=3^2/u$.

5. Polychromatic behavior of DLs

When using broadband illumination the monochromatic irradiances provided by the diffractive lenses regarded so far are affected by chromatic dispersion, as shown in Fig. 5. In the case of DLs the subsidiary foci can be considered as an extended depth of focus for each wavelength and, as can be seen, they partially overlap with the other ones creating an overall extended depth of focus, which should be less sensitive to the chromatic aberration than the conventional Fresnel kinoform lens. In this section we analyze this hypothesis.

Following the conventional approach, the behavior of a DL under broadband illumination can be evaluated in terms of the tristimuli values [18] computed along the optical axis

$$\begin{aligned}
 X &= \int_{\lambda_2}^{\lambda_1} I(r=0, z; \lambda) S(\lambda) \tilde{x} d\lambda; & Y &= \int_{\lambda_2}^{\lambda_1} I(r=0, z; \lambda) S(\lambda) \tilde{y} d\lambda; \\
 Z &= \int_{\lambda_2}^{\lambda_1} I(r=0, z; \lambda) S(\lambda) \tilde{z} d\lambda;
 \end{aligned}
 \tag{9}$$

where $S(\lambda)$ is the spectral distribution of the source and $(\tilde{x}, \tilde{y}, \tilde{z})$ are the three sensitivity chromatic functions of the detector and (λ_1, λ_2) represent the considered wavelength interval. In particular, in the assessment of visual systems $(\tilde{x}, \tilde{y}, \tilde{z})$ are usually the sensitivity functions of the human eye (CIE 1931) and the axial response is normally expressed in terms of the axial illuminance Y and the axial chromaticity coordinates x, y ,

$$x = \frac{X}{X+Y+Z}; \quad y = \frac{Y}{X+Y+Z};
 \tag{10}$$

In computing Eqs. (9) and (10) we considered 41 monochromatic irradiances numerically evaluated for equally spaced wavelengths ranging from 380 nm to 780 nm. The standard illuminant C was used as spectral distribution of the source. The result is shown in Fig. 6. Clearly, the axial illuminance for the DL [Fig. 6(a)] has an increased depth of focus compared with the kinoform Fresnel [Fig. 6(b)]. The degree of achromatization is evident in the display of the chromaticity [Fig. 6(c)]. In this figure we have computed the chromaticity curve for the axial points around the main focus: $0.8 < z/f < 1.3$. The open circle in this figure represents the $z=f$ for the design wavelength ($\lambda=550$ nm) of both zone plates. The triangles and squares represent $z/f=0.8$ and $z/f=1.3$, respectively. It can be observed that there are slow chromaticity variations for the DL and that the whole curve is closer to the point representing the white illuminant.

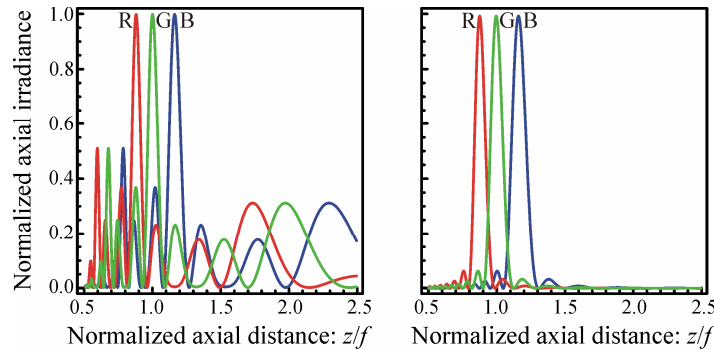


Fig. 5. Normalized irradiance vs. the axial coordinate u obtained for a DL (left) and for its associated Fresnel kinoform lens for three wavelengths R=650 nm; G=550 nm; and B=480 nm. In all cases $S=2$.

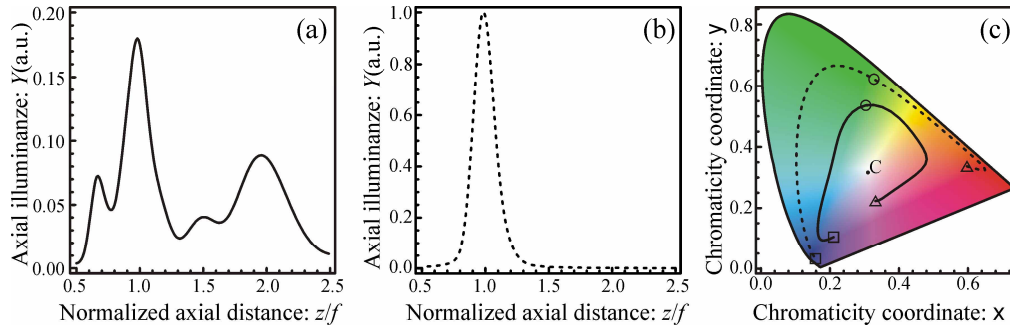


Fig. 6. Polychromatic axial illuminance computed (a) for a DL and (b) for its associated Fresnel kinoform lens. The chromaticity of both curves is shown in (c); the continuous line corresponds to the DL and the dashed line to the Fresnel kinoform.

6. Conclusions

A new type of pure phase DOEs, coined “devil’s lenses”, has been introduced. To avoid the absorption losses that characterize amplitude fractal zone plates and to improve their diffraction efficiency the phase function for a typical DL has a quadratic-fractal blazed profile. It is shown that the distribution of the surface grooves of these fractal lenses is obtained through the “devil’s staircase” or Cantor function. The focusing properties of DL have been analyzed and compared with those corresponding to a conventional Fresnel kinoform lens. When highly monochromatic sources are available the irradiance along the optical axis provided by a DL presents a single fractal focus with a characteristic fractal profile which results in a certain degree of axial superresolution for the main axial lobe. The minima appearing side by side around this lobe present transverse doughnut modes. The particular structure of the focal volume provided by DLs could be profited to develop optical tweezers, to trap particles of two different indexes, ones in the bright zones and the others in the dark core. Interestingly, DLs offer other advantages under polychromatic illumination. In fact, we have shown that they provide a widening in the axial illuminance and a reduction in the chromaticity distribution in comparison with the conventional Fresnel kinoform lens. The net result is an increase in the polychromatic depth of focus. Therefore, the potential uses of DLs are numerous in applications where a high depth of field is desirable but where the illumination sources are wideband. These applications cover different scientific and technological areas that use diffractive optics ranging from soft X-ray microscopy to THz imaging.

Acknowledgments

We acknowledge the financial support from: Grants DPI 2006-8309 and MTM 2004-06015-C02-01, Ministerio de Ciencia y Tecnología, Spain; Grant GV/2007/239, Generalitat Valenciana, Spain; Programa de Incentivo a la Investigación UPV 2005, Universidad Politécnica de Valencia, Spain.